Available online at www.sciencedirect.com
SCIENCE DIRECT®
Journal of Sound and Vibration 278 (2004) 63–81
JOURNAL OF SOUND AND VIBRATION
www.elsevier.com/locate/jsvi

Non-linear simulation of single pass perforated tube silencers based on the method of characteristics

A.I. Abd El-Rahman*, A.S. Sabry, A. Mobarak

Mechanical Power Department, Faculty of Engineering, Cairo University, Giza, Egypt

Received 23 January 2003; accepted 25 September 2003

Abstract

A quasi-one-dimensional characteristic based non-linear model for unsteady compressible flow is used to simulate the flow in single-pass perforated tube silencers. The flow in both short and long concentric tube resonators is simulated for both low and high-pressure excitation. The temporal solution is first transferred into the frequency domain using FFT, and then processed by the two-microphone technique in order to evaluate the transmission loss. Derivations of required equations, which are used to implement the method of characteristics along with the mathematical formulation of length corrections and different boundary conditions, are presented. The results obtained are compared with previously published experimental and numerical work, showing, in most cases, better agreement with the experimental data.

1. Introduction

Single-pass concentric tube resonators are widely used as acoustic silencing elements to attenuate noise exiting from the exhaust system of internal combustion engines. Composed of a perforated pipe with a surrounding cavity, they have received much attention due to their practical importance and simple geometry.

Earlier studies have pursued the lumped analysis [1,2] or zero-dimensional analysis, in which mechanically vibrating systems along with electrical analogies were used to describe the resonator behaviour. Such analysis is appropriate as long as the wavelength is larger than all element characteristic dimensions. At high frequency, lumped analysis failed to predict accurately the resonator behaviour and has been replaced by a one-dimensional (1-D) approach, when better

*Corresponding author.
E-mail addresses: arahman@eng.cu.edu.eg (A.I. Abd El-Rahman), ashraf_sabry@crown-eng.com (A.S. Sabry).

0022-460X/$ - see front matter © 2003 Elsevier Ltd. All rights reserved.
doi:10.1016/j.jsv.2003.09.062

results were achieved [3]. Sound attenuation in basic reactive silencers was then predicted in the frequency domain using linear acoustic theory [4].

In linear theory, low-pressure levels were maintained, and both friction and heat transfer were neglected. Sound attenuation has been predicted through the determination of the transmission matrix. Sullivan and Crocker [5] were the first to attempt to simulate the flow in perforated pipes in which the holes were modelled by considering the momentum equation in the radial direction under linear hole conditions. Sullivan [6] then proposed a new segmentation method to account for the holes. Many analytical and numerical decoupling techniques were carried out in order to enhance the prediction of sound attenuation by tracking both the mean flow and the variable perforate impedance along the duct [7–9]. A time domain approach was then used by Chang and Cummings [10] in examining the performance of perforated silencers. Although the governing equations were linearized, a non-linear hole model has been developed with the help of experimental coefficients to account for such non-linearity.

Unlikely, engine noise incorporates high-amplitude pressure oscillations that could not be modelled by linear theory for the simple reason that harmonics generated would be ignored and their effect would be eclipsed by the linearization of governing equations. A non-linear gas dynamic model [11–15] has the ability to account for high noise levels together with hole non-linearity, provided that such model is coupled with accurate numerical technique. Selamet et al. [16] developed a non-linear model in the time domain using a finite difference method based on the control volume approach. Greatly influenced by the work of Sullivan and Crocker [5], Dickey et al. [17] have employed frequency domain experimental data to account for hole non-linearity.

More recently, Dickey and Selamet [18] studied acoustic non-linearity of a circular duct. The relationship between pressure difference and flow rate across the hole was characterized in terms of equivalent length and hole resistance. Finally, Dickey et al. [19] used a time domain computational approach to investigate the behaviour of perforated tube silencers at high sound levels, employing a lumped parameter model for perforates based on experimentally empirical expressions for the equivalent length and hole resistance.

The analysis of the acoustic behaviour of a perforated tube silencer has been confronted by two main difficulties. The first difficulty is modelling the complex behaviour of flow through the perforations taking into consideration their non-linear effect. The second difficulty is to adopt a powerful computational tool that retains the equations in their non-linear form. The objective of this paper is to present a new simulation technique, based on the method of characteristics. Despite being first order accurate, the method of characteristics is able to retain system non-linearity, as well as accurately implementing the different boundary conditions, especially duct branching and anechoic termination. Two corrections are presented in order to increase the accuracy of the numerical solution, while the perforations model follows that proposed by Onorati [20] with only slight modifications.

In the present work, the solution proceeds in the time domain, and the attenuation characteristics are predicted in terms of transmission loss, employing the two-microphone technique, described by Chung and Blaser [21]. Both short and long concentric resonators are modelled. Computational predictions are compared with the published data of Selamet et al. [16] and Chang and Cummings [10].

2. Computational approach

2.1. The differential equations

The continuity, momentum and energy equations for quasi-1-D compressible flow, may be written as follows [22]:

$$\frac{\partial \rho}{\partial t} + \frac{\partial}{\partial x}(\rho u) + \frac{\rho u}{A}\frac{\mathrm{d}A}{\mathrm{d}x} = 0, \tag{1}$$

$$\frac{\partial}{\partial t}(\rho u) + \frac{\partial}{\partial x}(\rho u^2 + p) + \frac{\rho u^2}{A}\frac{\mathrm{d}A}{\mathrm{d}x} = -f\rho, \tag{2}$$

$$\frac{\partial}{\partial t}\left\{\rho\left(h - \frac{p}{\rho} + \frac{u^2}{2}\right)\right\} + \frac{\partial}{\partial x}\left\{\rho u\left(h + \frac{u^2}{2}\right)\right\} + \frac{1}{A}\left\{\rho u\left(h + \frac{u^2}{2}\right)\right\}\frac{\mathrm{d}A}{\mathrm{d}x} = \rho q. \tag{3}$$

The effects of wall friction f and heat transfer q are represented by specifying the friction factor C_f and the Stanton number St, defined by

$$C_f = \frac{1}{4}\frac{fd}{u|u|}, \tag{4}$$

$$St = \frac{1}{4}\frac{qd}{C_p|u|(T_w - T_o)}, \tag{5}$$

where C_p, T_w and T_o are the specific heat, wall temperature and stagnation temperature, respectively. The variables p, ρ and h are eliminated from the left-hand side of Eqs. (1)–(3) in favour of the sound speed, a and the entropy, s; then, substantial derivatives S, M and N are introduced as

$$S \equiv \frac{\partial}{\partial t} + u\frac{\partial}{\partial x}, \tag{6}$$

$$M \equiv S - a\frac{\partial}{\partial x}, \tag{7}$$

$$N \equiv S + a\frac{\partial}{\partial x}. \tag{8}$$

The physical meaning of operators S, M and N can be interpreted as the variation with time along a characteristic, of slope $1/u$, $1/(u-a)$ and $1/(u+a)$, respectively. The Riemann variables on which M and N will operate are defined as follows:

$$m \equiv a - \left(\frac{\gamma+1}{2}\right)u, \tag{9}$$

$$n \equiv a + \left(\frac{\gamma+1}{2}\right)u. \tag{10}$$

Through mathematical manipulations, the final differential equations can be written as

$$Mm = E - F\frac{\partial s}{\partial x} + H, \tag{11}$$

$$Nn = E + F\frac{\partial s}{\partial x} - H, \tag{12}$$

$$Ss = G, \tag{13}$$

where

$$E \equiv \left(\frac{\gamma - 1}{2}\right)\left[\frac{\gamma}{a}(q + uf) - a\frac{u}{A}\frac{\mathrm{d}A}{\mathrm{d}x}\right], \tag{14}$$

$$F \equiv \frac{a^2}{2C_p}, \tag{15}$$

$$G \equiv \frac{R\gamma}{a^2}(q + uf), \tag{16}$$

$$H \equiv \left(\frac{\gamma - 1}{2}\right)f. \tag{17}$$

2.2. The integration scheme

Employing a finite difference grid as shown in Fig. 1, Eqs. (11)–(13) are integrated along the characteristic lines, yielding the values of m, n and s at each of the nodal points at time $t + \Delta t$ on the basis of their values at time t.

The slopes of characteristic lines are based on the local conditions at point 1, 2 and 3 for n, s and m, respectively, as shown in Fig. 1. Since both the slope and position of points 1, 2 and 3 are not yet known, linear interpolations are carried out to locate their positions. For instance, to locate the position of point 1, the following linear interpolation is carried out:

$$[u + a]_1 \Delta t = \delta x, \tag{18}$$

$$\left[(u + a)_{i-1,j}\frac{\delta x}{\Delta x} + (u + a)_{i,j}\left(1 - \frac{\delta x}{\Delta x}\right)\right]\Delta t = \delta x, \tag{19}$$

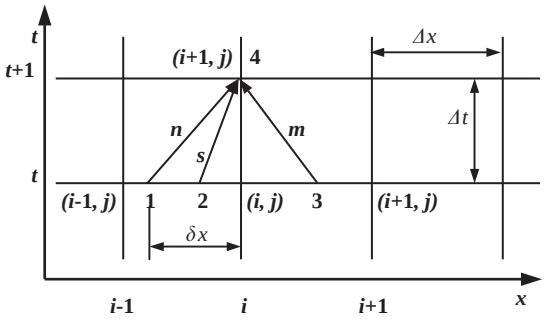

Fig. 1. Forward stepping procedure.

$$\delta x = 1 \Bigg/ \left[\frac{\dfrac{1}{\Delta x} - (u+a)_{i-1,j}\dfrac{1}{\Delta x}}{(u+a)_{i,j}} + \frac{1}{\Delta x} \right], \tag{20}$$

where δx is the distance between point 1 and the node (i,j). After locating points 1, 2 and 3, the integration is carried out in a backward difference scheme:

$$n_4 - n_1 = \int_1^4 \left[E + F\frac{\partial s}{\partial x} - H \right] \mathrm{d}t \approx \left[E + F\frac{\partial s}{\partial x} - H \right]_1 \Delta t t, \tag{21}$$

$$m_4 - m_3 = \int_3^4 \left[E - F\frac{\partial s}{\partial x} + H \right] \mathrm{d}t \approx \left[E - F\frac{\partial s}{\partial x} + H \right]_3 \Delta t t, \tag{22}$$

$$s_4 - s_2 = \int_2^4 G\,\mathrm{d}t \approx [G]_2 \Delta t t. \tag{23}$$

After m, n and s are calculated at each nodal point at time $t + \Delta t$, the procedure is repeated for time $t + 2\Delta t$ and so on. The stability criteria is given by the standard Courant condition

$$\Delta t \leqslant \frac{\Delta x}{|u| + a}. \tag{24}$$

It is worthwhile to mention here that the method of characteristics, as described, substantially suffers from two major drawbacks. It is first order accurate in space, due to linear interpolation carried out at the foot of the characteristic lines, and in time, because the time-stepping procedure in the integrating scheme is based on forward Euler technique.

Secondly, smearing of wave pattern at discontinuities due to the linear interpolation carried out at the foot of the characteristics. To overcome this artificial dissipation, it is recommended to ensure that the m and n characteristics are as diagonally as possible. This can be achieved by setting the time step as

$$\Delta t = \frac{\Delta x}{[|u| + a]_{\max}}. \tag{25}$$

This correction is repeated every time step, hence, Δt is a variable. By doing so, the interpolation ratio, given by $\delta x_{\max}/\Delta x$ where $\delta x_{\max}$ is the maximum distance between the foot of any characteristic and its respective grid point (i,j), approaches unity [23]. Thus, the need for linear interpolation is no longer important since points 1 and 3 will coincide with the grid points $(i-1,j)$ and $(i+1,j)$.

A significant reduction of the artificial dissipation is then guaranteed. It can be observed here that, unlike the other integrating scheme, where the time step has to be less than that of the Courant condition in order to minimize the truncation errors, the method of characteristics reaches its maximum accuracy when it runs under a unity Courant number.

It has been found [22] that an improved accuracy can be obtained by resorting to a re-evaluation step (correction step) for the integration scheme, utilizing the data that have already been derived at point 4 from the initial forward Euler stepping procedure. Inspired by the Euler-Trapezoidal method for integrating ordinary differential equations, Sallam et al. [23] proposed a

scheme to enhance the integration. Utilizing the data obtained at point 4 in Fig. 1, the position of point 1 is recalculated as follows:

$$\tfrac{1}{2}[(u+a)_1 + (u+a)_4]\Delta t = \delta x, \tag{26}$$

$$\frac{1}{2}\left[(u+a)_{i-1,j}\frac{\delta x}{\Delta x} + (u+a)_{i,j}\left(1-\frac{\delta x}{\Delta x}\right) + (u+a)_{i,j+1}\right]\Delta t = \delta x, \tag{27}$$

$$\delta x = 1 \Bigg/ \left[\frac{\dfrac{2}{\Delta t} - [(u+a)_{i-1,j} + (u+a)_{i,j}]\dfrac{1}{\Delta x}}{(u+a)_{i,j} + (u+a)_{i,j+1}}\right] \tag{28}$$

with the new value of n_4 calculated as

$$n_4 - n_1 \approx \left\{\left[E + F\frac{\partial s}{\partial x} - H\right]_1 + \left[E + F\frac{\partial s}{\partial x} - H\right]_4\right\}\Delta t. \tag{29}$$

The above mentioned correcting scheme could be repeated many times, until no further significant improvements are noticed. However, it is found that it is more accurate and more economical for computational time to choose a relatively finer grid and to apply the re-evaluation step only once [22].

3. Flow simulation

Simulation of the perforated tube silencer has been performed using an impedance tube for the overall configuration [16,17] as shown in Fig. 2. It consists of an acoustic source, acoustic element and a specific acoustic termination.

3.1. Boundary treatment

Apart from specifying the upstream system excitation, the purpose of boundary conditions is to provide the appropriate data, which are required by the method of characteristics, at the left- and right-hand sides for each duct in the flow field. The quasi-steady analysis can be employed to describe the instantaneous flow conditions into or out of the duct in which the unsteady flow occurs.

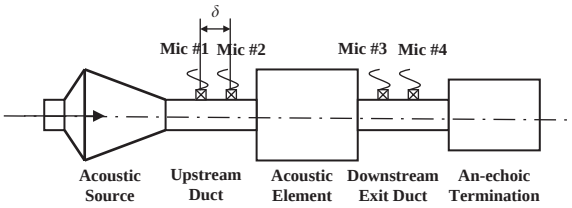

Fig. 2. Impedance tube configuration.

3.1.1. Excitation of duct system

White noise is a pressure signal that has a spectral content, which is uniformly distributed over the frequency band; it may excite the silencer with a constant amplitude pressure wave. A white noise approach [24] seems to be indispensable in the present study, due to great number of short ducts that are necessary to model the holes in the perforated tube and the cavity.

A significant reduction of the computational effort and computer running time is relatively achieved with respect to step by step frequency harmonic excitation. A fluctuating velocity, instead of a fluctuating pressure may be used to excite the silencer [14,15] where the source is modelled as an oscillating piston with a velocity u_{piston} given by

$$u_{\text{piston}} = u_m + \sum_{n=1}^{N} \Delta u \sin(n2\pi ft), \tag{30}$$

where, u_m is a specified mean flow velocity (equal to zero for null mean flow), Δu is the amplitude of the fluctuating input speed, f is the fundamental frequency and N is the number of harmonics. In terms of normalized variables

$$u'_{\text{piston}} = u'_m + \sum_{n=1}^{N} \Delta u' \sin(n2\pi ft). \tag{31}$$

Remembering that $u' = (n' - m')/(\gamma - 1)$ and by imposing the velocity disturbance at the upstream cross-section in characteristics form, it leads to

$$n' = m' - (\gamma - 1)\left[u'_m + \sum_{n=1}^{N} \Delta u' \sin(n2\pi ft)\right]. \tag{32}$$

A different approach can be used to model the input fluctuating signal, by imposing an oscillatory stagnation pressure p_o within an imaginary reservoir coupled to the duct system as

$$p_o = p_{o,m} + \sum_{n=1}^{N} \Delta p \sin(n2\pi ft), \tag{33}$$

where $p_{o,m}$ is the mean total imposed pressure, which may be set equal to or greater than the initial average pressure in the duct system and Δp is the amplitude of fluctuating input total pressure. Through further manipulation [14], assuming quasi-steady boundary condition and isentropic expansion from the reservoir to the first duct cross-section, Eq. (33) can be written in characteristics form as

$$\left(p'_{o,m} + \sum_{n=1}^{N} \Delta p' \sin(n2\pi ft)\right)^{(\gamma-1)/\gamma} = \left(\frac{m' + n'}{2}\right)^2 + \frac{\gamma - 1}{2}\left(\frac{n' - m'}{\gamma - 1}\right)^2. \tag{34}$$

This latter approach is probably more realistic, since the fluctuating pressure imposed in the external reservoir, is not forced to maintain such fluctuation at the first cross-section. Furthermore, it is suitable for achieving a non-zero mean flow excitation in the pipe system.

3.1.2. Acoustic termination

The present work simulates the anechoic (non-reflecting) silencer termination for sake of comparison and validation with experimental results of Selamet et al. [16] and Chang and Cummings [10]. The boundary condition for the anechoic termination at the duct exit has been proved to be the most suitable one to be implemented [25]. This is achieved by resorting to the method of characteristics adopted earlier, which is naturally well-suited to describe the interaction of incident and reflected waves at the boundaries.

The non-reflecting termination eliminates any effects of wave reflection downstream and results in transmission loss as a function of silencer geometry. Its condition [25] implies that there is no incoming wave at the duct exit, which is accomplished by reserving its amplitude, represented by the Riemann variable m', constant in time. In the work of Selamet et al. [15], the anechoic termination has been modelled as a long duct, with a viscous shear that is increasing along the duct, causing the travelling wave to be damped before reaching the open end, thus preventing its reflection at the atmospheric interface.

3.1.3. Closed end

For a closed end duct, the inward boundary condition is the zero velocity condition at the boundary. Thus, by assuming a rigid wall at the duct end (unity reflection coefficient), it can be easily proven that

$$m' = n' \tag{35}$$

3.2. Perforated tube silencer model

The model adopted for perforated tube silencer follows that proposed by Onorati [20], where branches of several ducts treated by the equal total enthalpy model of Corberan [26] have been considered to represent the flows in every single hole of the perforated duct section. Similarly to Onorati [20], a typical perforate is shown in Fig. 3a, which consists of perforated duct surrounded by a cavity liner, whereas the acoustically equivalent system of Fig. 3b is adopted to represent the flow across the holes, taking into account the effective porosity of the acoustic filter.

By means of an appropriate friction factor, the dissipative behaviour of the holes is introduced while the reactive one is accounted for by the addition of an appropriate length correction for the short ducts representing the holes. It is worth mentioning that for the case of zero mean flow and the low-pressure level (acoustic excitation) case, the dissipative effect related to holes would not be significant and the silencer behaviour is predominantly reactive. However, for high-pressure level excitation, the length correction should be modified to account for the accompanied non-linear flow behaviour as will be discussed in a later section. Also, the effect of non-zero mean flow on both length correction and friction factor has been considered.

Onorati [20] has pointed out that due to the large number of ducts to be simulated using his approach, it is important to reduce significantly the total number of ducts via a reasonable approximation. Such approximation assumes that each group of holes may be regarded as a single equivalent hole. Thus, the total computational running time is minimized without altering the porosity of the perforated duct. However, the length correction that was used was a function of the equivalent diameter instead of the geometrical hole diameter. It is important to note that this

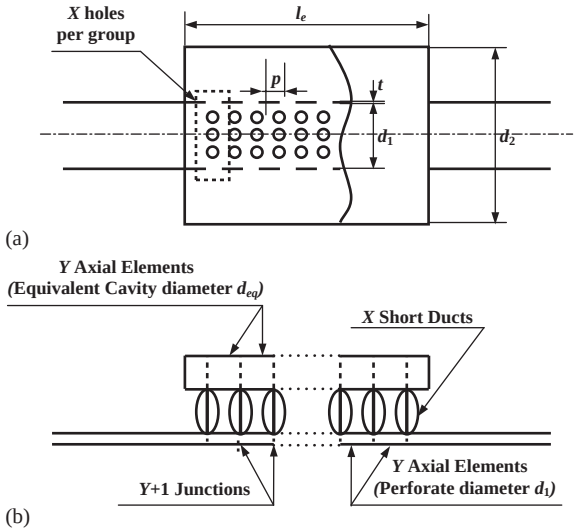

Fig. 3. (a) Typical single-pass perforated tube silencer company; (b) sketch of the acoustically equivalent system.

model has been validated against a zero mean flow case, and high porosity (26%) perforates and showed a good agreement with experimental results for acoustic excitation.

3.3. Perforated tube silencer model modification

In the present work, the model described earlier is studied and validated against different perforates with lower porosities. However, the authors recommend that the following modification must be taken into consideration in order to be able to extend successfully the applicability of this model to various types of perforated silencers with different porosities along with high pressure level excitation coupled with non-zero mean flow.

It is important to mention the fact that the adopted numerical method, based on the method of characteristics, is mainly non-linear. However, it still suffers the 1-D assumption of wave propagation. That is why a length correction was added to the original duct length to account for the three-dimensional (3-D) effect of actual wave propagation through discontinuities. Thus, whenever treating highly oscillating flow in holes, the length correction should be updated to describe well the reactive behaviour of hole non-linearity that was based on the linear approach.

In the present work and for relatively low porosity perforated duct (2% to 5%), the value of $0.8d_h$ was used for the length correction, similar to Onorati [20], in case of long resonator. However, it was found that the length correction of $0.7d_h$ is more appropriate for short resonator in seeking better agreement with the available experimental results. This is in accordance with Davies et al. [1] who stated that the length correction would reach a maximum of 0.8 times the diameter of the hole. Such correction values were adopted in the present simulation in case of acoustic excitation (i.e., linear behaviour). Note that the values of length correction vary neither in time nor in space going through adjacent holes.

However, for high-pressure amplitude excitation (hence, high oscillating hole velocity), the dominant non-linear behaviour would sharply reduce the corrective length. Eventually, the length

correction depends on the instantaneous hole velocity, and hence vary in time as well as in space. But, according to Dickey and Selamet [18] and Dickey et al. [19], approximate treatment is still possible, leading to constant value of length correction over a cycle (time invariant). At relatively high-pressure level excitation (greater than 160 dB, ref = 20 μPa), the corrective length drops to $0.4d_h$ for most of the frequencies considered in the simulation. This value is used in the present work as an average value in all holes.

On the other hand, for non-zero mean flow, this length correction slightly decreases (case of grazing flow) as expressed by Cummings [27]

$$\frac{l}{l_o} = \left(1 + 0.6\frac{t}{d_h}\right)\exp\left[-\left(\frac{U_*}{ft} - 0.12\frac{d_h}{t}\right)\Big/\left(0.25 + \frac{t}{d_h}\right)\right] - 0.6\frac{t}{d_h}, \tag{36}$$

where f is the signal fundamental frequency, l is the length correction with mean flow, l_o is the length correction without mean flow, t is the hole length (perforated duct wall thickness) and U_* is determined from the relationship $U_* = U_m\sqrt{C_f}/2\sqrt{2}$ (U_m is the mean grazing flow velocity in the pipe).

It is important to mention that the dissipative behaviour has been accounted for by choosing a suitable friction factor in the viscous term of the governing equations for the ducts representing the holes. The friction factor used in the present work was equal to 0.005 for both the linear and non-linear simulations in accordance with Onorati [13], whereas for non-zero mean flow simulation, a friction factor of 0.01 has been introduced in the computation.

Moreover, when further approximation is considered for gathering the group of holes in a single equivalent hole, it has been found that no further change in the length correction should be applied. That means that the length correction retains its values of $0.7d_h$ for short resonator and $0.8d_h$ for long resonator. Such result is not surprising, since the length correction should depend on the real geometrical diameter of the holes, unlike the equivalent diameter in the former model proposed by Onorati [20].

In the present work, Benson's constant pressure model [28] is adopted for two reasons. The first reason is the simplicity acquired by the lower number of ducts per junction. The second reason is that it is quite appropriate as long as the flow velocities through the junction are low, which is the condition in most of the cases studied. Nonetheless, Corberan's time consuming model [26] would be a better choice in cases where a large number of holes and high velocities cases are encountered.

3.4. Benson model for duct branches

In the present work, the boundary conditions for all ducts branches follows those described by Benson [28], where a constant static pressure has been assumed in each of the pipe communicating with the branch. Applying the conservation of mass and pressure equilibrium, Benson [28] developed a simple algorithm for unsteady compressible homentropic flow in a junction with any number of joining ducts. Benson's model has been implemented and leads to excellent agreement with experimental results, particularly, for zero mean flow. Benson showed that

$$\lambda_{\text{unknown}_r} = \sum_{r=1}^{n}\left[\left(\frac{2A_r}{\sum_{r=1}^{n} A_r}\right)\lambda_{\text{known}_{rr}}\right] - \lambda_{\text{known}_r}, \tag{37}$$

where A_r = cross-sectional area of the rth pipe communicating the junction, $\lambda_{\text{unknown}_r}$ = unknown, time dependent, characteristic quantity (i.e., m' or n') at the boundary of the rth duct and λ_{known_r} = known, time dependent, characteristic quantity (i.e., m' or n') at the boundary of the rth duct.

4. Transmission loss calculation

This study presents the attenuation in terms of the transmission loss TL, defined as the ratio of sound power entering the silencer from the acoustic source to the exiting sound power and it is then an invariant property of the element:

$$TL(f) = 10 \log_{10} \frac{W_i(f)}{W_t(f)}. \tag{38}$$

In order to evaluate the transmission loss of the acoustic elements, the two-microphone technique presented by Chung and Blaser [21] is used. The theory beyond this technique involves the decomposition of the acoustic wave into its incident and reflected components using the frequency response relation between the acoustic pressures at two locations on the tube wall, as shown in Fig. 2. It is important to note that the two microphones spacing δ must be chosen (as shown in Fig. 2) such that [21]

$$\delta \leqslant C_o/2f_m, \tag{39}$$

where f_m is the maximum exciting frequency.

5. Planar wave propagation

In this section, it is intended to state the condition by which the assumption of 1-D flow is preserved. That is because the implemented numerical technique is limited only to planar wave propagation. Doing so, the frequency must remain below the cut-on frequency of the first higher order mode. For the general case, the first possible mode is the diametrical mode [2], which may continuously propagate, yielding a cut-on frequency:

$$f_c \leqslant \frac{1.841 C_o}{\pi d}, \tag{40}$$

where d is the inner diameter of the perforated pipe (low porosities) or the outer cavity (higher porosities). However, for cases in which both inlet and outlet tubes are centred on the axis of the silencer (radially symmetric configuration), plane wave approximation will be then accurate up to cut-on frequency of the first circularly symmetric or radial mode [2] given by

$$f_c \leqslant \frac{3.832 C_o}{\pi d}. \tag{41}$$

6. High-amplitude excitation

6.1. Hole non-linearity

It should be stressed that the simulation against acoustic excitation, as will be shown later in Section 7, represents only one of the steps that has been taken to validate the non-linear gas dynamic model as well as the adopted model for perforated tube and the boundary conditions. In the limit of low sound pressure level and zero mean flow, the dissipative effect related to holes would not be significant and the silencer behaviour is predominantly reactive.

As the sound pressure level is increased, the flow velocity through the hole increases, until flow separation occurs and vorticity is generated. Since very little of the vortical energy is restored back to the pressure field, both convective and viscous terms of the governing equations represent energy losses that occur in the flow through perforations, and result in the dissipative behaviour of the perforated silencer. It is interesting to note that Chang and Cummings [10] based their numerical model on linearized governing equations, except for the holes whose non-linear behaviour was expressed by resistance variables. Empirical relations were developed, in favour of experimental data, to represent hole resistance.

In the present work, a suitable effective length correction for the hole duct presents the effect of the hole's non-linearity. As shown in Section 3.3, the length correction for high sound pressure level, drops to $0.4d_h$ [18,19].

6.2. Grazing flow

A grazing flow is defined as the mean flow tangential to the perforation interface. In such case, it is likely to assume that the mean flow exists only inside the perforated duct of Fig. 3a. Sullivan and Crocker [5] showed that grazing flow tends simultaneously to decrease the peak transmission loss and increase the frequency of the primary peak, effects similar to those of high-amplitude excitations. It is important to note that holes' non-linearity may be eclipsed, even at high-amplitude pressure excitation, if grazing flow speeds were high enough to largely restore linear behaviour [10]. In the present work, for non-zero mean flow simulation, a friction factor of 0.01 has been introduced in the computation.

7. Silencer results

The first part of this section presents the computational results for perforated tube silencer geometries for both short and long concentric tube resonators, introducing acoustic (low pressure level) excitation and zero mean flow. For such linear simulations, comparisons are performed with numerical and experimental data of Selamet et al. [16]. The second part is devoted for the non-linear simulations, where predicted results of transmission loss from the present numerical approach are compared with the numerical and experimental data of Chang and Cummings [10]. The perforated silencers considered in this paper consist of three single-pass configurations. The silencers include both short and long concentric resonators. Table 1 shows the basic geometries of the single-pass perforated tube silencers.

7.1. Geometries

One short and two long resonators, the geometry and dimensions of which are shown in Fig. 3a and Table 1, respectively, were simulated. The first two resonators have dimensions and area porosity σ (averaged between the inner and outer surfaces of the perforated tube) consistent with the silencer used in the linear simulation of Sullivan and Crocker [5] and Selamet et al. [16]. The third resonator has dimensions and area porosity consistent with the silencer used in the non-linear simulation (high-amplitude excitation) of Chang and Cummings [10]. All the three resonators are considered evenly perforated over the central tube as shown in Fig. 3a.

The inner diameter of both upstream and downstream tubes for the first two resonators are 4.859 cm, while for the third resonator, the inner diameter of both upstream and downstream tubes are equal to the inner diameter of the perforated pipe. As mentioned earlier, the positions at which the four signals are extracted are absolutely arbitrary. According to Chung and Blaser [21], the distance between the two microphones upstream does not even need to equal that of the downstream pair. The two-microphones' spacing in each pair is chosen to be 3.556 cm, satisfying Eq. (39). The distances between the microphones' locations and silencer are kept at a minimum of 2.5 cm.

To verify the non-linear gas dynamic technique, the numerical approach is first applied to resonators R-1 and R-2, with linear acoustic excitation, just to validate the perforated tube silencer model, boundary conditions and length corrections used in this simulation. Results are compared with the work of Selamet et al. [16]. The non-linear effects (high-amplitude oscillations) are then investigated using resonator R-3, where results are compared with the work of Chang and Cummings [10].

7.2. Resonator R-1

As a short resonator, it is defined as having the volume controlled resonance at a frequency below the first axial modal frequency of the cavity ($f_1 = C_o/2l_e$). Such a case may be regarded as a volume controlled resonator. It is to be noted that at a higher frequency, a transition in behaviour occurs that results in length controlled resonance. Comparison of the present model results with both experimental and numerical data of Selamet et al. [16] is included in Fig. 4. Overall, the present results show slightly better agreement with experimental data, especially between 1700 and 2200 Hz.

7.3. Resonator R-2

A long resonator is defined as having the volume controlled resonance at a frequency above the first axial modal frequency of the cavity ($f_1 = C_o/2l_e$). Such a case may be regarded as a length

Table 1
Dimensions of the three resonators

R	l_e (cm)	d_1 (cm)	d_2 (cm)	t_{wall} (cm)	Porosity (σ)	d_{hole} (cm)
R-1	6.67	5.08	7.62	0.079	0.037	0.249
R-2	25.72	5.08	10.15	0.079	0.02	0.249
R-3	25.4	2.66	6.35	0.34	0.0397	0.318

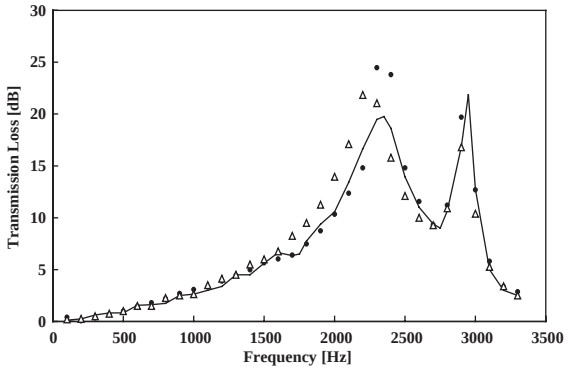

Fig. 4. Transmission loss of short concentric resonator (R-1): •, numerical (Present); △, numerical (Selamet et al. [16]); —, experiment (Selamet et al. [16]).

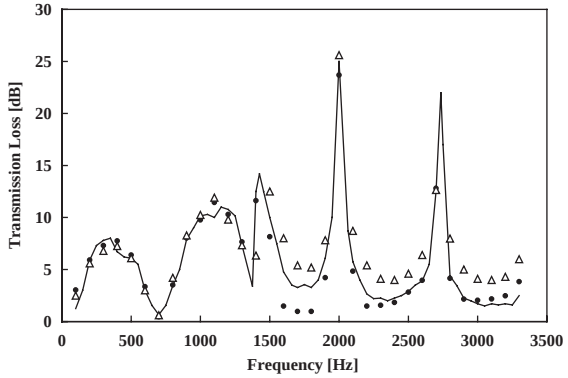

Fig. 5. Transmission loss of long concentric resonator (R-2): •, numerical (Present); △, numerical (Selamet et al. [16]); —, experiment (Selamet et al. [16]).

controlled resonator. Similar to the short resonator, the results of the transmission loss of the element are compared with both the experimental and numerical results of Selamet et al. [16]. As shown in Fig. 5, the present results are in general in better agreement with the experimental results.

7.4. Resonator R-3

In this section, another more sophisticated case will be treated to generalize the application of the model, with some consideration given to high-amplitude wave motion and mean flow, associated with a real ICE. For comparative purposes, the case studied by Chang and Cummings [10] is modelled in the present work. Contrary to the earlier treated cases, the input pressure spectrum is modelled by means of total oscillating pressure (Eq. (33)), instead of oscillating velocity applied at the upstream cross-section. It is worth mentioning that the amplitude of the fluctuating input total pressure in the above-mentioned equation (Δp) was taken to be equal to the peak acoustic pressure (167 dB). Using such an approach, the mean flow can be easily maintained

by introducing total input pressure higher than the initial reference pressure in the duct system. Also, an anechoic termination is chosen at the downstream exit cross-section area.

In this case, a typical perforated pipe of circular section separates the central channel carrying the gas flow from the surrounding cavity. The central perforated tube was drilled with 120 circular holes, which were distributed in eight staggered rows. The test was carried experimentally and simulated numerically [10] for two fundamental frequencies of the input signal (151 and 178 Hz). The complex acoustic signal of each frequency constitutes ten harmonics.

7.4.1. Low-mean grazing flow

A prediction for an intense periodic signal with a peak of 167 dB, a fundamental frequency of 151 Hz and low mean flow Mach number of 0.018 is presented. Using the two-microphone method of Chung and Blaser [21], the transmission loss is predicted in the present work and is compared with the experimental and numerical results of Chang and Cummings [10], as shown in Fig. 6. Generally, better agreement with previous experimental data is achieved. Thus, the inherent capability of the present non-linear gas dynamics model is explicitly confirmed.

7.4.2. High mean grazing flow

In this section, a prediction for an intense periodic signal with a peak of 167 dB, a fundamental frequency of 178 Hz and average mean flow Mach number of 0.193 is examined. The comparison in Fig. 7 suggests that the present model captures the general behaviour of transmission loss. The present results show fair agreement with the experimental data, especially, when compared with Chang and Cummings [10] predicted results.

Although grazing flow, as indicated in Section 6.2, induces the restoration of system linearity, the prediction of transmission loss in case of strong non-linearity proved to be more representative than the prediction in the case of grazing flow. This conclusion emphasizes the ability of the present technique to simulate a real engine with high-amplitude noise source.

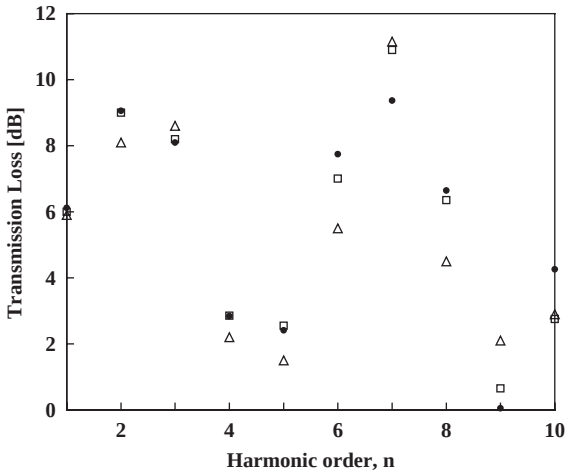

Fig. 6. Transmission loss of long resonator (R-3). Fundamental frequency = 151 Hz, Mach no. = 0.018. ●, numerical (Present); △, numerical (Chang and Cummings [10]); □, experiment (Chang and Cummings [10]).

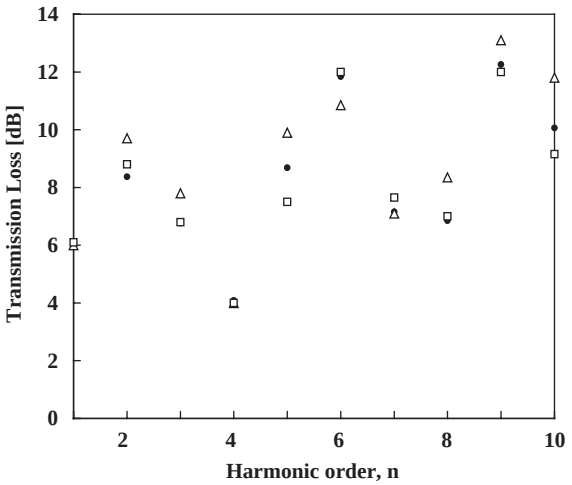

Fig. 7. Transmission loss of long resonator (R-3). Fundamental frequency = 178 Hz, Mach no. = 0.193. ●, numerical (Present); △, numerical (Chang and Cummings [10]); □, experiment (Chang and Cummings [10]).

The overall agreement between the calculated and measured data, for both the cases of low and high mean flow, is certainly satisfactory for most of the harmonics of the imposed fundamental frequency. However, some discrepancies are observed due to the numerical viscosity, which is necessary to damp frequency oscillations beyond the pulse of each peak pressure.

It is worth mentioning that turbulence and vortex shedding noise, which is certainly present in the measurement, is not taken into account in the simulation. Such noise is noticeable in the grazing flow case [29,30] due to high mean flow and relatively low amplitude of the pulse noise. Discrepancies between predicted and measured may be attributed to that part as well, which is remarkable for the fifth and tenth harmonics as shown in Fig. 7.

8. Concluding remarks

The first order accuracy of the method of characteristics, resulting from linear interpolation between grid points at the foot of the characteristic in the space domain, has been improved by introducing a unity courant number, thus maintaining the characteristic lines as diagonally as possible. In addition, introducing a one correction step that uses the Euler-Trapezoidal integration scheme has enhanced the integration of Riemann variables along the characteristic lines. In addition, the large time taken by a computer run, especially in perforated silencers where large number of ducts are simulated, has been greatly reduced to a minimum by resorting to the input white noise signal.

Complex silencers can be modelled satisfactorily by a non-linear gas dynamic technique using suitable acoustical equivalent elements, quasi-steady boundary conditions and by inserting corrective lengths at discontinuities to overcome the limitations of the assumption of 1-D wave propagation. It has been shown that the model suggested by Onorati [20], which treats the flow through the holes along the perforate duct with high porosity, can also be successfully applied to a

low-porosity perforated duct, provided that slight modifications regarding the length correction to take account of the 3-D effect, especially in case of non-zero mean flow are considered.

Finally, the present technique proved its ability to simulate the non-linear attenuation effects. Comparison with the experimental work of Chang and Cummings [10] justified such a claim. Thus, such a model is strongly recommended to be used to predict the attenuation effects of perforated tube silencers, which exist in the exhaust systems of internal combustion engines.

Acknowledgements

The authors would like to thank Prof. A. Selamet of the Department of Mechanical Engineering, Ohio State University, OH, (USA) and Prof. A. Onorati of the Department of Energetics, Politecnico di Milano, Milan (Italy) for providing their papers at the authors' request. Thanks are also due to the valuable discussion with Prof. A. Onorati and the referees' comments.

Appendix A. Nomenclature

A	cross-sectional area
a	sound speed
C_f	friction factor
C_o	mean sound speed
d	pipe diameter
E, F, G, H	variables as defined in Eqs. (14)–(17)
f	frequency or fiction force per unit mass of fluid
h	enthalpy
k	wave number, $2\pi f/C_o$
M	modified substantial derivative
m	Riemann variable, $a-((\gamma-1)/2)u$
N	modified substantial derivative
n	Riemann variable, $a+((\gamma-1)/2)u$
p	absolute pressure
q	heat transfer rate through the duct into fluid per unit mass of fluid
S	substantial derivative
St	Stanton number
s	entropy or second
T	temperature
TL	transmission loss
t	time or thickness
u	fluid flow velocity

Greek symbols

ρ	density
δ	two-microphone spacing

δx distance from node (i, j)
Δ finite increment of subject variables
Δf frequency band width
λ wave length

Subscripts

i incident component
m mean value
o stagnation value
t transmitted component

Superscripts

$'$ normalized value

References

[1] D.D. Davis Jr., G.M. Stokes, D. Moore, G.L. Stevens Jr., Theoretical and experimental Investigation of Mufflers with comments on engine-exhaust Muffler design, National Advisory Committee for Aeronautics Report No. 1192, 1954.
[2] L.J. Eriksson, Higher order mode effects in circular ducts and expansion chambers, *Journal of the Acoustical Society of America* 68 (2) (1980) 545–550.
[3] D.F. Ross, A finite element analysis of perforated component acoustic systems, *Journal of Sound and Vibration* 79 (1) (1981) 133–143.
[4] P.O.A.L. Davies, Practical flow ducts acoustics, *Journal of Sound and Vibration* 124 (1) (1988) 91–115.
[5] J.W. Sullivan, J. Crocker, Analysis of concentric-tube resonators having unpartitioned cavities, *Journal of the Acoustical Society of America* 64 (1) (1978) 207–215.
[6] J.W. Sullivan, A method for modeling perforated tube Muffler components, I. Theory, II. Applications, *Journal of the Acoustical Society of America* 66 (3) (1979) 772–788.
[7] K. Jayaraman, K. Yam, De-coupling approach to modeling perforated tube Muffler components, *Journal of the Acoustical Society of America* 69 (2) (1980) 390–396.
[8] M.L. Munjal, K.N. Rao, A.D. Sahasrabudhe, Aero-acoustic analysis of perforated Muffler components, *Journal of Sound and Vibration* 114 (2) (1986) 173–188.
[9] K.S. Peat, A numerical decoupling analysis of perforated pipe silencer elements, *Journal of Sound and Vibration* 123 (2) (1988) 199–212.
[10] I.J. Chang, A. Cummings, A time domain solution for the attenuation, at high amplitudes, of perforated tube silencers and comparison with experiment, *Journal of Sound and Vibration* 122 (2) (1988) 243–259.
[11] T. Morel, J. Morel, D.A. Blaser, Fluid dynamic and acoustic modeling of concentric tube resonators/silencers, SAE, No. 910072, 1991.
[12] S.M. Sapsford, V.C.M. Richards, D.R. Amelee, T. Morel, M.T. Chapell, Exhaust system evaluation and design by Non-Linear Modeling, SAE, No. 920686, 1992.
[13] A. Onorati, Prediction of the acoustical performances of Muffling pipe systems by the methods of characteristics, *Journal of Sound and Vibration* 171 (3) (1994) 369–395.
[14] A. Onorati, G. Ferrari, Calculation of complex silencer performances by non-linear fluid dynamic simulation models, *Proceedings of the International Conference Inter-Noise* '94, Yokohama, Japan, 1994, pp. 1631–1634.
[15] A. Selamet, N.S. Dickey, J.M. Novak, A time domain computational simulation of acoustic silencers, *Journal of Vibration and Acoustics* 117 (1995) 323–331.

[16] A. Selamet, N.S. Dickey, J.M. Novak, A time domain based computational approach for perforated tube silencers, *Proceedings of Noise Congress '93: Noise Control in Aero-Acoustics*, Leuven, Belgium, 1993, pp. 291–296.
[17] N.S. Dickey, A. Selamet, J.M. Novak, Multi-pass perforated tube silencers: a computational approach, *Journal of Sound and Vibration* 211 (3) (1998) 435–448.
[18] N.S. Dickey, A. Selamet, Acoustic non-linearity of a circular hole: an experimental study of the instantaneous pressure/flow relationship, *Noise Control Engineering Journal* 46 (3) (1998) 97–107.
[19] N.S. Dickey, A. Selamet, J.M. Novak, The effect of high-amplitude sound on the attenuation of perforated tube silencers, *Journal of the Acoustical Society of America* 108 (3) (2000) 1068–1081.
[20] A. Onorati, Non-linear fluid dynamic modeling of reactive silencers involving extended inlet/outlet and perforated ducts, *Noise Control Engineering Journal* 45 (1997) 35–51.
[21] J.Y. Chung, D.A. Blaser, Transfer function method of measuring in-duct acoustic properties, I: Theory, II: Experiment, *Journal of the Acoustical Society of America* 64 (3) (1980) 907–913, 914–921.
[22] J.A. Kentfield, *Non-steady, One Dimensional, Internal, Compressible Flows, Theory and Applications*, Oxford University Press, Oxford, 1993.
[23] K.A. Sallam, A.S. Sabry, M.A. Serag-Eldin, M.A. Fouad, Characteristic based non-linear simulation of reactive silencers, *International Congress on Fluid Dynamics & Propulsion*, Cairo, Egypt, 1996.
[24] A. Onorati, A white noise approach for rapid gas dynamic modeling of IC engine silencers, *Third International Conference on Computers in Reciprocating Engines & Gas Turbines*, London, 1996.
[25] K.W. Thompson, Time-dependant boundary conditions for hyperbolic systems, II, *Journal of Computational Physics* 89 (1990) 439–461.
[26] J.M. Corberan, A new constant pressure model for N-branch junctions, *Proceedings Institute of Mechanical Engineers, Part D: Journal of Automobile Engineering* 206 (1992) 117–123.
[27] A. Cummings, The response of a resonator under a turbulent boundary layer to a high amplitude non-harmonic sound field, *Journal of Sound and Vibration* 115 (2) (1987) 321–328.
[28] R.S. Benson, A simple algorithm for multi-pipe junction in non-steady homentropic flow, *Journal Mechanical Engineering Science* 17 (1) (1975) 40–41.
[29] G. Ferrari, A. Onorati, Determination of silencer performances and radiated noise spectrum by 1-D dynamic modeling, *Proceedings of the XXV FISITA Congress*, Beijing, China, Paper No. 945135, 1994.
[30] A. Onorati, Numerical simulation of exhaust flows and tailpipe noise of a small single cylinder diesel engine, SAE, Paper No. 951755, 1995.